RSC Advances

ROYAL SOCIETY OF CHEMISTRY

www.rsc.org/advances

RSC Advances

ARTICLE

Fabrication and characterization of collagen coated electrospun Poly (3-hydroxybutyric acid)-gelatin nanofibrous scaffold as a soft bio-mimetic material for skin tissue engineering applications

Received 00th January 20xx,
Accepted 00th January 20xx

DOI: 10.1039/x0xx00000x
www.rsc.org/

Giriprasath Ramanathan[a], Sivakumar Singaravelu[a], M. D. Raja[a], Naveen Nagiah[b], P. Padmapriya[c], K. Ruban[c], Krishnasamy Kaveri[c], Natarajan. T. S[d], Uma Tiruchirapalli Sivagnanam[a]*, Paramasivan Thirumalai Perumal[e]*

The wound healing is a global health care problem, the use of suitable dressing material that finds repairing the damaged skin tissue by means of nanofibrous scaffold with traditionally important medicine. The ideal wound dressing material should mimic the function of extracellular matrix with its improved physiochemical, biological and antimicrobial property. In this study, the significance feature of collagen coated electrospun Poly(3-hydroxybutyric acid)-gelatin nanofibrous scaffold with bioactive *Coccinia grandis* extract (CPE) meets the requirement defined for wound dressing material. The nanofibrous scaffold with collagen has an attraction of fibroblast for increased cell adhesion and proliferation. The fabricated nanofibrous scaffold with collagen were physio-chemically characterized using Fourier transform infrared (FTIR) spectroscopy, scanning electron microscopy (SEM) and showed acceptable antibacterial property with both Gram positive and Gram negative bacteria. The thermal and *in vitro* stability of the nanofibrous scaffold were studied and possessed to have more stability that suitable for wound dressing material. The nanofibrous scaffold supports good swelling property with better porosity for oxygen permeability. The mechanical property of the nanofibrous scaffold showed a Young's modulus of 2.99±0.16 MPa. The biocompatibility of the nanofibrous scaffold exhibits increased cell adhesion and proliferation of both NIH 3T3 fibroblast and Human keratinocytes (HaCaT) cell line. The *in vitro* fluorescence staining of the nanofibrous matrix using Calcein AM and DAPI exhibits the cell material interaction of the collagen coated nanofibrous scaffold corresponds to the increased cell adhesion and proliferation. This approach with nanofibrous scaffold coated with collagen is capable to provide as a promising tool in skin tissue engineering and useful as a wound dressing material in skin tissue engineering application.

Introduction

The advancement of tissue engineering provides the combination of the multidisciplinary field, for the development of matrix scaffold enriched with therapeutic products for the repair, restoration and regeneration of the damaged cells or tissue [1]. The use of nanofibrous scaffold in the tissue engineering application involves the support of the cells by mimicking the function of extracellular matrix (ECM) [2]. The nanofibrous scaffold has excellent structural similarity towards the ECM with its ability to provide a substratum for the cell migration into the defective sites [3]. The efficiency of the nanofibrous scaffold in wound healing has several advantages to retain certain properties to allow good oxygen permeability, flexibility, high surface to volume ratio and biocompatibility with sequential reformation in the wound healing process [4]. The triple helical structure with high glycine amino acid content of the collagen is most important for attachment and proliferation of cells thought the collagen matrix with efficiently by mimicking the function of the native cells [5, 6]. The collagen coated nanofibrous scaffold finds its significant function over the extracellular matrix (ECM) by its matrix scaffolding and resistance to give, cell-cell interaction [7],

a. Bioproducts Lab, CSIR-Central Leather Research Institute, Chennai-600020, Tamilnadu, India. E-mail: suma67@gmail.com; Tel: + 91 44 24420709; Fax: +91 44 24911589
b. Department of Mechanical Engineering, University of Colorado, Boulder, USA.
c. Department of Virology, King Institute of Preventive Medicine and Research, Guindy, Chennai-600032, Tamilnadu, India.
d. Conducting Polymers Lab, Department of Physics, Indian Institute of Technology Madras, Chennai, India
e. Organic Chemistry Division, CSIR-Central Leather Research Institute, Adyar, Chennai-600020, Tamilnadu, India. E-mail: ptperumal@gmail.com; Fax: +91 44 24911539; Tel: + 91 44 24437223

cell-ECM interaction [8] and high mechanical property [9,10]. The electrospun biomaterial enhances the ability of nanofibre due to the high surface to volume ratio with its porous structure, which favors both the physical and biological properties of the nanofibrous scaffold [11].

The Poly(3-hydroxybutyric acid) (PHB), a hydrophobic polymer with excellent application in the field of medicine for its biodegradability and biocompatibility [12]. The combination of PHB has been used for various products such as sutures, stents, nerve guides and wound dressing material [13]. The PHB is a common metabolite in all higher living organisms, which provides the proof for the non-toxicity [14]. The electrospinning of collagen causes denaturation to form gelatin, a major constituent of the ECM [15]. The gelatin with its excellent biocompatibility, non-antigenicity, and adhesiveness properties has wide application in biomedical and pharmaceutical fields [16].

The traditionally important compound from the plant possesses a bioactive constituent that acts as a conventional medicine. The ancient villagers used numerous crude extract for the healing of skin diseases and wounds. The present world always relies on the indigenous traditional medicine for their primary health needs [17]. *Coccinia grandis* commonly known as ivy gourd, all the plant parts were traditionally important against skin related problems. The bioactive *Coccinia grandis* leaf extract (CPE) has enhanced antioxidant property to treat ulcers, treatment of diabetes, and antibacterial activity [18].

The biomaterial with all ideal properties cannot be attained alone with natural and synthetic polymers. The individual polymers have their drawback associated with improved physical, mechanical and biological properties. In order to overcome these drawbacks with individual polymer, electrospinning of nanofibrous scaffold with blending of two polymers with a surface coating of collagen has been explored to assimilate the all properties to in design of nanofibrous scaffold for tissue engineering application [19].

In this context, some researchers have given that the gelatin have been blended with various synthetic polymers such as poly(e-caprolactone) (PCL) [20, 21, 22], polyvinyl alcohol (PVA) [23, 24], Poly(L-lactide acid) (PLLA) [25], polyglycolic acid (PGA) [26] and Poly(3-hydroxybutyrate-co-3-hydroxyvalerate) (PHBV) [27] for various tissue engineering applications. However the use of Poly(3-hydroxybutyric acid) (PHB) blended with gelatin and uniform coating of collagen over the nanofibrous scaffold were thoroughly investigated with biocompatibility, cell adhesion, cell proliferation, cell attachment and spatial distribution of the cells throughout the nanofibrous matrix with NIH 3T3 fibroblast and Human keratinocytes (HaCaT) cells.

In current research driven towards the fabrication, characterization and application of collagen coated bioactive nanofibrous scaffold for tissue engineering. The Poly(3-hydroxybutyric acid) (P) and gelatin (G) are electrospun to form a nanofibrous scaffold with the incorporation of bioactive extract (CBE) to provide antibacterial property. Further, the developed PG-CPE nanofibrous scaffold was coated with *Arothron stellatus* collagen (COL) solution to make as a PG-CPE-COL scaffold as a wound dressing material in tissue engineering application.

Materials and methods

Materials

The *Arothron stellatus* fish was collected from the Bay of Bengal in Nagapattinam, Tamil Nadu, India. The leaves of *Coccinia grandis* (Cucurbitaceae) were collected from Tiruvarur, Tamilnadu, India and authenticated with the help of a plant taxonomist Dr. N. Veerappan, Associate Professor, Sir Theayagaraya College, Chennai, Tamilnadu, India. Poly(3-hydroxybutyric acid), Gelatin, 1,1,1,3,3,3 hexafluoro-2-propanol, 3-(4,5-dimethylthiazol-2-yl)-2,5-diphenyl tetrazolium bromide (MTT), 4,6-diamino-2-phenylindol (DAPI), Calcein AM, Dulbecco's modified Eagle's medium (DMEM), Fetal calf serum (FCS), and supplementary antibiotics for tissue culture were purchased from Sigma Aldrich, India. The NIH 3T3 fibroblast and Human keratinocytes (HaCaT) cell lines was obtained from the National Centre for Cell Science (NCCS), Pune, India. The rest of the chemicals and culture wares were purchased from Sigma Aldrich, unless specified otherwise.

Methods

Extraction of collagen from *Arothron stellatus* skin

The fish skin obtained was washed, chopped and fat removed were soaked in 0.5 M acetic acid for 3 days. The loosened thin epidermal layer was removed from the skin. After which swollen dermal skin pieces were homogenized with 0.5 M acetic acid using the Homogenizer (Ultra Turax T-50, IKA Werke, Germany). The homogenized skin was centrifuged at 8000 rpm for 30 min at 4°C. The salt precipitated was dialyzed against 0.1 M acetic acid solution to obtain *Arothron Stellatus* skin collagen. The collagen was washed with distilled water, and then lyophilized (Operon Co., Korea) [28].

Extraction of *Coccinia grandis* plant extracts (CPE)

Healthy and fresh leaves of *Coccinia grandis* were collected and surface cleaned with Millipore filtered water, shade dried, and finely powdered with the help of an electric blender. An ethanol extract was prepared by subjecting 10 g of the finely powdered leaf in a

Soxhlet apparatus. The aqueous extract was concentrated using rotary evaporator apparatus under reduced pressure and the CPE was stored at 4°C [29].

Electrospinning nanofibrous scaffold containing plant extract coated with collagen (PG-CPE-COL)

To prepare PG-CPE nanofibre scaffold, 4 wt% concentration of polymer solution were prepared by dissolving 0.4g of Poly(3-hydroxybutyric acid) and gelatin in 10 mL of 1, 1, 1,3,3,3 hexafluoro-2-propanaol. The dissolved solution obtained after constant stirring for 12 hours were mixed to obtain a blended solution of Poly (3-hydroxybutyric acid) and gelatin in 1:1 ratio with 0.5 mg/ml of CPE was electrospun with 24 G needle connected to the positive terminal of the high voltage DC power supply (ZEONICS, Bangalore, India). The polymer solution were extruded at 1.5ml/h using a computer controlled syringe pump and was subjected to an electric potential of 1.5 kV/cm. the fibers were collected onto the grounded aluminum substrate around a rotary drum placed at a distance of 12 cm perpendicular to the needle. The 4 wt% collagen solution in 0.1 M acetic acid was prepared. Further, the electrospun PG-CPE scaffold was prepared collagen solution and was dried at room temperature (37°C) to get the PG-CPE-COL scaffold. The prepared scaffolds were stored at room temperature until further use [14].

Characterization

Fourier Transform Infrared Spectra (FTIR)

Fourier transform infrared (FTIR) measurements were carried out to determine the functional groups present in the prepared PG, PG-CPE and PG-CPE-COL nanofibrous scaffolds. The spectra were measured at a resolution of 4 cm^{-1} in the frequency range of 4000–600 cm^{-1} using ABB 3000 spectrometer with Grams as the operating software [14]. Thermogravimetric analysis (TGA) and Differential scanning calorimetry (DSC) analysis of the nanofibrous scaffolds were done using universal V4.4A TA instruments [30].

Scanning electron microscope (SEM)

The scaffolds were mounted on brass studs and were gold coated using an ion coater (Emitech brand). The surface morphology of the scaffolds was visualized using (F E I Quanta FEG 200 - HRSEM) operating at an accelerating voltage of 5– 20 kV. 50 different fibers were measured using the UTHSCA Image tool software to determine the average diameter of the fibers for different concentrations of the polymer solution.

The cell morphology of the nanofibrous scaffold was observed using SEM. The cell-seeded scaffolds were rinsed with PBS after three days of cell seeding and fixed using 10% neutral formalin buffer for 5 h at 4ºC. For dehydration, the scaffolds were dehydrated through a series of graded alcohol solution and then dried [30].

Porosity

The porosity of the nanofibrous scaffold was determined *via* liquid displacement method using ethanol as the displacement liquid because of its easy penetration through the pores of the scaffolds and which will not induce shrinking or swelling as a non solvent of the polymers [31]. A known weight (W) of the sample was immersed in a graduated cylinder containing a known volume (V_1) of ethanol. The sample were kept in ethanol for 5 min, and then a series of brief evacuation – repressurization cycles were conducted to force the ethanol in to the pores of the scaffold. The process was repeated until the air bubbles stops. The total volume of the ethanol and the ethanol-impregnated scaffolds were then recorded as V_2. The difference in the volume was calculated by (V_2–V_1). The scaffolds impregnated in ethanol were removed from the cylinder, and the residual ethanol volume was recorded as V_3. The porosity of the dressing was obtained by the following equation

$$\text{Porosity } (\%) = \frac{(V_1 - V_3)}{(V_2 - V_3)} \text{x } 100 \qquad \text{---1}$$

***In vitro* enzymatic degradation**

Nanofibrous scaffolds were exposed to collagenase enzyme (Sigma #C0773) to assess biological stability of the material and its degradation rate. Known weight of each sample in triplicate was taken and they were air dried overnight at room temperature. All the samples were exposed with the collagenase enzyme (100 units/ml) for 24h at 37°C (pH 7.4). After 24h, all the test samples were removed from the incubator, dried by blotting and left to air drying for 24 h at room temperature. Percentage of weight loss and final mass were calculated as simple ratio. Enzyme solutions were prepared in a phosphate buffer solution (PBS, pH 7.4). The extent of biomaterial degradation was determined gravimetrically through weight loss [32].

Swelling behavior

The *in vitro* swelling behavior of the nanofibrous scaffold were done by cutting the scaffold into a square piece (10 × 10 mm^2) and immersing it in PBS (pH 7.4) at room temperature until the film reached swelling saturation. The weights of the scaffolds were after removing the surface wetness by using filter paper. The equilibrium-swelling ratio was calculated by using the following equation.

$$\text{Swelling } (\%) = \left(\frac{W_1 - W_0}{W_0}\right) \times 100 \qquad \text{---2}$$

where, W_0 and W_1 are the initial and the final weights of the film, respectively [33].

Tensile strength measurement

All the scaffolds were cut into dumb-bell shaped specimens (100 x 16 mm^2), prepared, and load-elongation measurement was measured using a universal testing machine (INSTRON model 1405) according to Vogel at an extension rate of 5 mm/min [30].

***In vitro* Biocompatibility, Cell adhesion and proliferation studies**

Cell viability of the nanofibrous scaffolds were performed using MTT assay. The NIH 3T3 fibroblast and Human Keratinocytes (HaCaT) cell line were grown on the PG-CPE-COL nanofibrous scaffold placed in 24 well plates (Corning, NY) and maintained in DMEM with 10% fetal calf serum supplemented with penicillin (120 units per mL), streptomycin (75 mg/mL^{-1}), gentamycin (160 mg/mL^{-1}), and amphotericin B (3 mg/mL^{-1}) at 37°C at a density of 5×10^4 cells/mL and then incubated over a time interval for 24 h, 72h and 7th day in a humidified atmosphere of 5% CO_2. Cells cultured in blank wells were used as control [11]. After 24h, 72h and 7th day the culture medium was replaced with a serum-free medium containing 10 µL of 3-(4,5-dimethylthiazol-2-yl)-2,5-diphenyl tetrazolium bromide (MTT) and incubated at 37°C for 4 h in a humidified atmosphere of 5 % CO_2. The medium was aspirated and then 500 µL/well of dimethylsulfoxide (DMSO) was added to dissolve the formazan needles with slow agitation for 10 min to yield a bluish purple solution. The absorbance of the dissolved solution was measured at 570 nm using Universal Microplate Reader [33].

The cell attachment and proliferation of both NIH 3T3 fibroblast and Human keratinocytes (HaCaT) cell line were quantified for live cell and cell nuclei staining assay at regular time intervals (6, 12, 24 and 48 hours), the medium was removed and the cells were fixed with 4% Paraformaldehyde and washed with PBS for several times. Furthermore, each cell was first stained with DAPI to visualize the cell nuclei. For achieve this aim, the cell were treated with DAPI solution (1.0 mg/ mL) for 15 min at 37°C, then washed again with PBS several times. Then Calcein AM solution (2 µM; 400 µl) was added and incubated for 30 min at 37°C, Then the plates with scaffold were washed with PBS for several times and viewed at fluorescence microscope (EVOS FLoid Cell Imaging Station, Thermo fisher SCIENTIFIC, USA) [34, 35].

Bacterial culture and antimicrobial activity

In this study, two bacterial strains were used, including one Gram positive bacteria *Staphylococcus aureus* (ATCC 11632) and one Gram negative bacteria *Escherichia coli* (ATCC 10536). All bacterial cultures were subcultured and maintained aseptically. The antimicrobial activity of the scaffolds were evaluated using modifying agar well diffusion method. About 100 µL [10^5 CFU (colony forming units)] of each bacterial culture was spread on the agar surface (Muller-Hinton agars) using a sterile glass spreader. Then, the plates were incubated for 24h at 37ºC. The antibacterial activity was evaluated by measuring the zone of inhibition against the test organism [35].

Statistical analysis

All the experiments were conducted in triplicate. Results are presented as mean ± S.D. (n = 3). ANOVA (analysis of variance) and student's t-test were done to determine the significant differences among the groups. The observed differences were statistically significant when $p < 0.05$.

Results and discussion

Characterization

Fourier Transform Infrared Spectra (FTIR): The structural modification due to the blending of PG with CPE in electrospinning were confirmed using FTIR spectra were depicted in Figure 1(a). There were no apparent peaks of the solvent were noticed during the electrospinning process. All corresponding peaks were of PG, PG-CPE and PG-CPE-COL found in the IR spectrum. The entire scaffold showed characteristic amide I (1600-1660 cm^{-1}), amide II (~1550 cm^{-1}) and amide III (1320-1220 cm^{-1}) absorption bands of gelatin [36]. The characteristic absorption band of PHB was seen at the range 1720-1740 cm^{-1} and 1270-1280 cm^{-1} that corresponds mainly due to the ester carbonyl group, and -CH group respectively [37]. The PG-CPE-COL scaffold showed the characteristic absorption band of amide A (3100–3600 cm^{-1}), exhibits a broad band associated with N-H stretching vibration of hydrogen bonded amide groups. The amide I (1600-1660 cm^{-1}) corresponds to the carbonyl

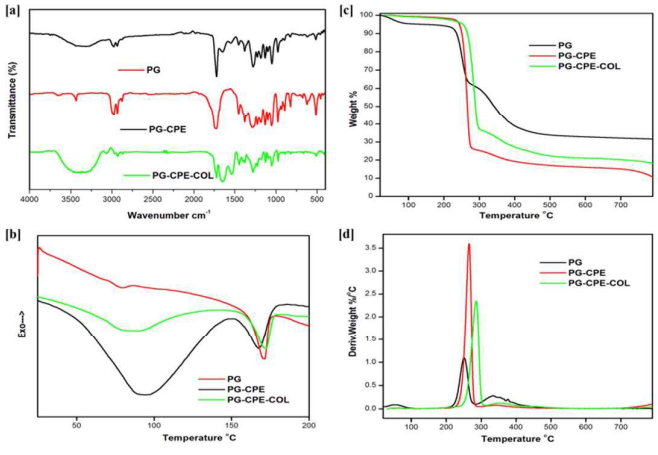

Figure 1 (a) FTIR spectra, (b) DSC, (c) TGA and (d) DTA of nanofibrous scaffold

Table1 Thermal properties of electrospun nanofibrous scaffolds

Sample Name	$T_{-5\%}$ (°C)	T_{max1} (°C)	T_{max2} (°C)	T_d (°C)	T_m (°C)	ΔH_m (J/g)	ΔH_d (J/g)
PG	197.3	265.6	350.6	77.7	173.13	161.53	-1.47
PG-CPE	198.1	252.8	334.7	93.30	167.97	-11.53	-116.3
PG-CPE-COL	200.2	287.1	353.2	81.5	171.95	-30.98	-89.33

group, which is offered within the triple helix structure in the secondary structure of protein. The N-H bending and N-H stretching vibration referred to the amide II (~1550 cm^{-1}) and amide III (1320-1220 cm^{-1}) respectively [33]. The presence of phenolic deformation and carbonyl group at 1414 cm^{-1} and 1740 to 1630 cm^{-1} respectively corresponds to the alkaloids in the both CPE blended nanofibrous scaffold [38]. All scaffold exhibit C-H stretching absorption bands at 2987 cm^{-1} and 2933 cm^{-1} corresponds to the CH_2 and CH_3 in PHB and gelatin scaffolds [14]. The IR spectrum data contain all the characteristic peaks correspond to the entire nanofibrous scaffolds.

Thermal analysis

The thermogravimetric analysis (TGA) and differential thermal analysis (DTA) of the nanofibrous scaffolds were shown in Figure 1(c) and (d). The scaffold can be utilized for tissue engineering and biomedical application as it reveals satisfactory thermal stability. The single step weight loss was observed between 250 and 300°C, which were apparent from the T_{max} and $T_{-5\%}$ values from the Table 1. The characteristic change in endothermic peaks of the nanofibrous scaffold was presented in Figure 1(b). The DSC reveals the denaturation temperature of collagen in the PG-CPE-COL nanofibrous scaffold exhibit at 81.5°C. The PG, PG-CPE and PG-CPE-COL scaffolds showed endothermic peaks at 173.13°C, 167.97°C and 171.95°C respectively was due to the degradation of the scaffold. The collagen coated PG-CPE scaffold showed a significant interaction with both CPE and PG with an increase in the denaturation temperature [33, 39].

Scanning Electron Microscopy (SEM)

Figure 2(a-c) and Figure 2 (d-f) depicts the SEM image and photographic images of nanofibrous scaffold PG, PG-CPE and PG-CPE-COL. The average diameters of the fibers (Figure 2(g-i)) were approximately 240±30 nm. Incomplete evaporation of solvent was observed in collagen coated PG-CPE scaffold. In Figure 2 exhibited that collagen was highly interconnected small micro fibrils onto the fibers of the PG-CPE scaffold as a collagen matrix embedded nanofibrous scaffold. The coalescence of nanofibrous scaffolds showed clearly visible fibers at the junctions, added more advantageous to contribute the enhancement of the tensile strength of the nanofibrous scaffold. Overall the fibrous nature of the scaffold will improve the cell attachment and permeability of the oxygen [14, 40].

Porosity

The PG and PG-CPE nanofibrous scaffold showed about 72% porosity with decreased rate when compared to collagen coated scaffold (Figure 3). This was due to the strong adherence of the collagen matrix in between the nanofiber matrix.

Therefore, PG-CPE-COL exhibited only 64.3% of porosity. The material used for the wound dressing should accomplish porous nature for oxygen and nutrient exchange. In soft tissue engineering, scaffold materials should have the porous nature for nutrient and gas exchange [31, 32].

In vitro enzymatic degradation

The *in vitro* enzymatic stability of nanofibrous scaffold was assessed to measure the degradation rate and biological stability against the collagenase enzyme. In Figure 4 shows that the PG and PG-CPE nanofibrous scaffold exhibited 71.29% and 60.8% weight loss

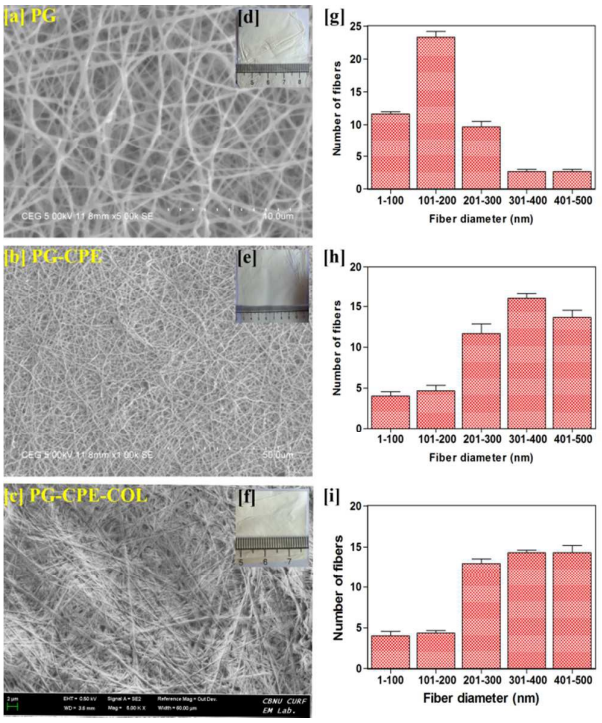

Figure 2 (a-c) SEM micrograph of the nanofibrous scaffold with their fiber diameter (g-i) and (d-f) insight showing the photographic images of the nanofibrous scaffold

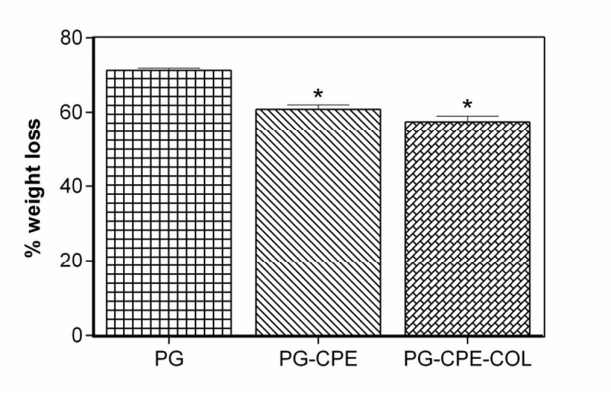

Figure 3 Porosity measurement of the nanofibrous scaffold (*p < 0.05; data presented are mean ±SD, n =3)

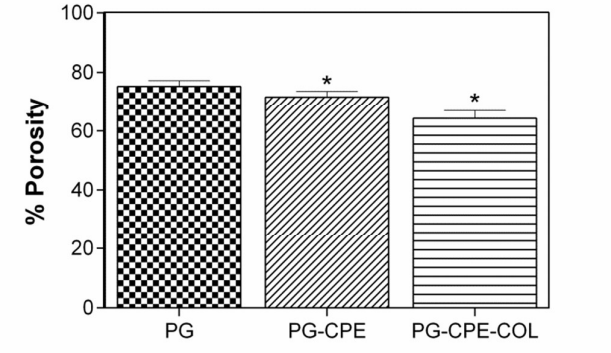

Figure 4 in vitro enzymatic degradation of the nanofibrous scaffold (*p < 0.05; data presented are mean ±SD, n =3)

respectively. Whereas the PG-CPE-COL nanofibrous scaffold showed a 57.4% weight loss. The existence of collagen matrix causes an increased reduction in the biodegradability of the PG-CPE-COL nanofibrous scaffold. Thus the presence of collagen decreases the percentage of biostability of the scaffold, but this property will aid in cell proliferation and attachment when it acts as the dressing material [41].

Swelling behavior

It is important to fabricate the nanofibrous scaffold with good swelling behavior to absorb the wound exudates and to keep the wound region dry and free from infection. The swelling behavior of the PG-CPE-COL nanofibrous matrix (Figure 5) has shown better swelling behavior and attains saturation after 24h. Only collagen coated nanofibrous scaffold showed an increase in swelling than other scaffold due to the surface bounding of the collagen to the nanfibrous matrix. However the CPE binds with gelatin during the electrospinning process and form PG-CPE nanofibrous scaffold with increased swelling index than PG scaffold. Figure 5 depicts the swelling behavior of the nanofibrous scaffold. The initial swelling

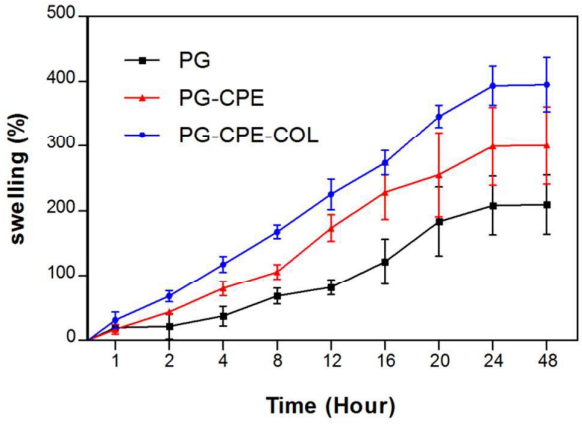

Figure 5 Swelling behavior of the nanofibrous scaffold

of the collagen makes the nanofibrous scaffold more sufficient to enhance the oxygen permeability with increase porosity of the scaffold, thereby improves the wound healing efficiency. [33, 42].

Tensile strength measurement

The nanofibrous scaffold needs to be robust enough with prominent mechanical property for both handling and sterilization, before it has to be applied onto the wound surface. The strength of the fibrous scaffold was mainly due to the property of the material used in the fabrication. The mechanical property based on the uniaxial tensile strength was conducted and the results were given in Table 2. The PG and PG-CPE scaffold exhibited relatively same Young's modulus of 2.84±0.07 MPa and 2.83±0.32 MPa respectively. The collagen coated scaffold showed significantly high tensile strength with Young's modulus of 2.99±0.16 MPa. The increase in the Young's modulus of the PG-CPE-COL was due to the enhanced entanglement of the collagen over the PG-CPE scaffold provided for tissue engineering nanofibrous scaffold [43].

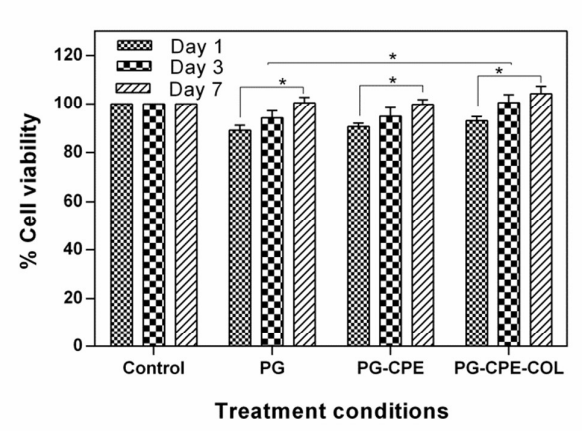

Figure 6 In vitro biocompatibility of NIH 3T3 fibroblast cell line over 1 day, 3 day and 7 day using MTT assay scaffold after 7 and 14 days. The data are represented as the means± standard deviation; n = 3 (*P < 0.05).

Table 2 Tensile properties of the nanofibrous scaffolds

Sample name	Mean Tensile Strength (MPa)	Mean Elongation at Break (%)	Mean Extension at Maximum Load (mm)	Mean Young's modulus (MPa)
PG	13.7±0.7	15.8±0.6	4.8±0.2	2.84±0.07*
PG-CPE	13.1±0.6	15.3.±0.5	4.6±0.3	2.83±0.32*
PG-CPE-COL	14.8±0.4	16.9±0.5	4.9±0.3	2.99±0.16*

(*p < 0.05; data presented are mean ±SD, n =3)

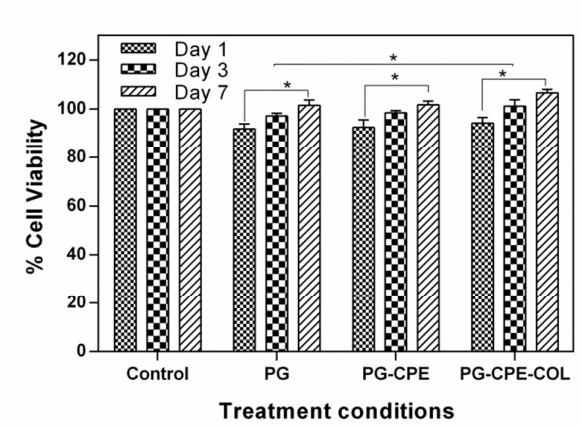

Figure 7 In vitro biocompatibility of Human (HaCaT) keratinocytes cell line over 1 day, 3 day and 7 day using MTT assay. The data are represented as the means± standard deviation; n = 3 (*P < 0.05).

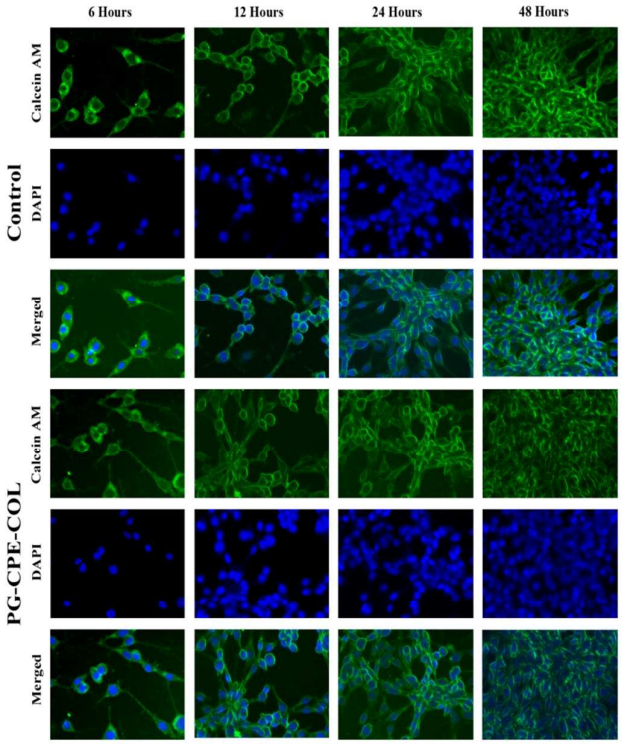

Figure 8 Calcein AM - DAPI fluorescence staining images of NIH 3T3 fibroblast cell adherence and proliferation onto the PG-CPE-COL nanofibrous scaffold in comparision with control at various time interval of 6, 12, 24 and 48 hours. The scale bar measures in 100 µm

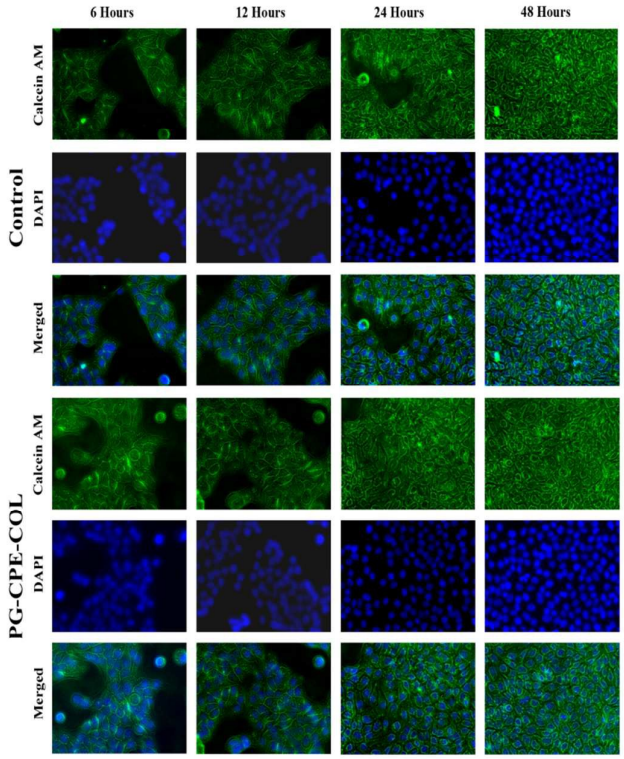

Figure 9 Calcein AM - DAPI fluorescence staining images of the Human (HaCaT) keratinocytes cell adherence and proliferation onto the PG-CPE-COL nanofibrous scaffold in comparision with control at various time interval of 6, 12, 24 and 48 hours. The scale bar measures in 100 µm

***In vitro* Biocompatibility, Cell adhesion and proliferation studies**

In order to ensure the tissue engineering application of the nanofibrous scaffolds with better biocompatibility was determined by MTT assay. The percentage of cell viability of the scaffolds with NIH 3T3 fibroblast and Human keratinocytes (HaCaT) cells after 1st day, 3rd day and 7th day was exhibited in Figure 6 and Figure 7. The PG-CPE-COL showed a significant increase in the cell viability of the scaffold. It was noticed that the presence of collagen in the PG-CPE scaffold enhance the biocompatibility of the nanofibrous scaffold [43, 44].

The growth of fibroblast provides uniform spreading of cells with an increase in cell adhesion and proliferation in the nanofibrous matrix. Researchers found that unique property of the collagen matrix has attracted a certain type of cell types mainly fibroblast. The collagen coated nanofibrous scaffold exerts influence on the fibroblast

interaction with collagen matrix. For instance, Asaga *et al.,* [45] proposed the indirect interaction *via* cellular fibronectin between that fibroblast and collagen. However, the interaction not only depends on the collagen matrix and cells, but also has interaction between the groups of cells with the surrounding matrix. Which signifies that collagen emerges as the biomimetic in nature to emphasize the function of the extracellular matrix [46]. The high biocompatibility of the scaffold with a high degree of cell attachment in the scaffold was mainly due to the presence of fibroblast interaction with the collagen matrix [47, 48]. The cell proliferation and cell adhesion behavior of the NIH 3T3 fibroblast and keratinocytes cells on the surface of the nanofibrous matrix were assessed based on the four major steps with cell-material contact, cell-material interaction, cell attachment and spreading that will precede better biocompatibility [49].

In Figure 8 and Figure 9 both cells were specifically studied using the Clacein AM -DAPI fluorescence staining. Furthermore, Calcein AM was associated with the live cell imaging, whereas, DAPI was used to visualize the cells via cell nuclei staining over the nanofiber matrix. Both NIH 3T3 fibroblast and Human keratinocytes (HacaT) cell lines reveals good cell adhesion with increased in cell amount significantly compared to that of control cells. Both cells exhibit an increase in cell growth onto the PG-CPE-COL nanofibrous scaffold. Moreover, it was noted that collagen coating on the nanofibrous matrix was beneficial and aids to sustain cell adhesion with a major role in cellular process. However, PG nanofiber matrix frames support in achieving the cell adhesion to the material surface via intracellular focal adhesion, spreading, proliferation and differentiation by mimicking the function of the extracellular matrix. The fluorescence microscopic analysis and cell viability investigation were congruent with the cell attachment and proliferation results [50]. Ultimately, the both cells were well spread and anchored throughout the nanofibrous matrix, exhibiting a stretched morphology with increase in cell numbers. It is evident that increase in cell attachment and proliferation was occurred in both cells between 12h to 48h with the nanofibrous scaffold, which created the strong attachment with soft nanofibrous membrane.

Antimicrobial activity of the scaffolds

The antimicrobial activity of the nanofibrous scaffold was evaluated against two bacterial strains. The CPE in the scaffold found to undergo rapid neutralization of the plant compound in the wounded region and will not make a significant difference in the wound surface. Therefore scaffold without CPE did not form any zone when compared with the PG-CPE-COL scaffold was depicted in Figure 10 (a) and (b).

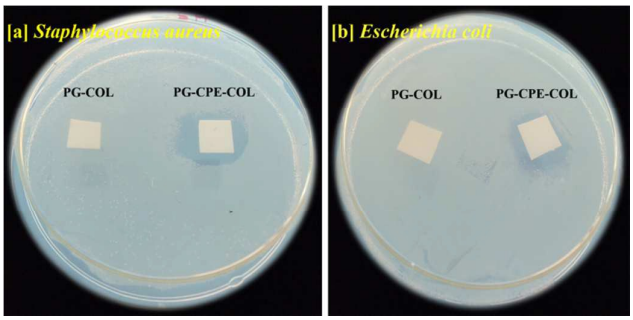

Figure 10 Antimicrobial activity of the nanofibrous scaffold (a) *Staphylococcus aureus* and (b) *Escherichia coli*

The PG-CPE-COL scaffold with 0.3 mg/10x10 mm^2 concentration of the CPE in the scaffold showed a clear zone of inhibition against both *Staphylococcus aureus* and *Escherichia coli*. The formation of clear zone implies that CPE has active inhibition to get prevent from infection at the wound site. This makes the PG-CPE-COL nanofibrous scaffold as a suitable dressing material in tissue engineering application [31, 34].

Conclusion

In this work, successful fabrication of PG-CPE-COL nanofibrous scaffold was obtained *via* electrospinning. The nanofibrous scaffold found to have good physiochemical property and fiber morphology. The swelling behavior and porosity of the scaffolds were found to be suitable for wound dressing material with better mechanical property. The antibacterial property of the scaffold against both Gram positive and Gram negative bacteria was enhanced by the presence of CPE, Which was compared with the scaffold without CPE. The *in vitro* fluorescence staining clearly exhibits the cell adhesion and proliferation of the cells onto the nanofibrous scaffold. The collagen supports in achieving better cell attachment over the nanofibrous matrix. Moreover the excellent attachment of fibroblast and keratinocytes over the nanofibrous scaffold demonstrates its potential substrate in skin tissue engineering application.

Acknowledgments

R. Giriprasath thanks the Council of Scientific and Industrial Research (CSIR) (award number 31/6(395)/2014-EMR-I), New Delhi, India, for providing the funds to carry out this study.

References

1. Chuanglong He, Wei Nie and Wei Feng, *J. Mater. Chem. B*, 2014, **2**, 7828.
2. N. Goonoo, A. Bhaw-Luximon and D. Jhurry, *RSC Adv.,* 2014, **4**, 31618.

3. R. Rajesh and Y. Dominic Ravichandran, *RSC Adv.,* 2015 , **5**, 41135.
4. Payam Zahedi, Iraj Rezaeian, Seyed-Omid Ranaei-Siadat, Seyed-Hassan Jafari and Pitt Supaphol, *Polym. Adv. Technol.*, 2010, **21**, 77–95.
5. In-Sung Yeo, Ju-Eun Oh, Lim Jeong, Taek Seung Lee, Seung Jin Lee, Won Ho Park and Byung-Moo Min, *Biomacromolecules,* 2008, **9**, 1106.
6. Eun Song, So Yeon Kim, Taehoon Chun, Hyun-Jung Byun, Young Moo Lee, *Biomaterials,* 2006, **27** 2951.
7. E. Reichenberger, B.R. Olsen, Cell Dev. Biol., 1996, 7, 631–638.
8. V. Ottani, D. Martini, M. Franchi, A. Ruggeri, M. Raspanti, Micron., 2002, **33**, 587–596.
9. J.M. Pachence, J. Biomed. Mater. Res., 1996, **33**, 35–40.
10. Marco Biondi, Francesca Ungaro, Fabiana Quaglia, Paolo Antonio Netti, Advanced Drug Delivery Reviews, 2008, **60** 229–242.
11. Young Won Koo, Hyeong jin Lee, Suji Kim, No-Joon Song, Jin-Mo Ku, Jae Hwan Lee, Chang Hyun Choi, Kye Won Park and Geun Hyung Kim, *RSC Adv.,* 2015, **5**, 44943.
12. Piras, A. M., Chiellini, F., Chiellini, E., Nikkola, L. and Ashammakhi N, *J. Bioact. Compat. Polym.,* 2008, **23**, 423.
13. Frier, T., Kunze, C., Nischan, C., Kramer, S., Sternberg, K., Sab, M., Hopt, U. T. and Schmitz, K. H, *Biomaterials.,* 2002, 23, **13**, 2649.
14. Naveen,N., Ramadhar, K., Balaji,S., Uma,T.S. , Natarajan, T.S. and Praveen, K.S, *Adv. Eng. Mat.,*2010, **12**, B380.
15. Dimitrios I. Zeugolis, Shih T. Khew, Elijah S.Y. Yew, Andrew K. Ekaputra, Yen W. Tong, Lin-Yue L. Yung, Dietmar W. Hutmacher, Colin Sheppard, Michael Raghunath, Biomaterials, 2008, **29**, 2293.
16. Chang Seok Ki, Doo Hyun Baek, Kyung Don Gang, Ki Hoon Lee, In Chul Um, Young Hwan Park, *Polymer,* 2005, **46**, 5094.
17. Anoja Priyadarshani Attanayake, Kamani Ayoma Perera WijewardenaJayatilaka, Chitra Pathirana, Lakmini Kumari, Boralugoda Mudduwa, *Asian Pac J Trop. Dis.* 2013, **3,** 460.
18. B. Deepti, K. Sasidhar, G. Sadhana, P. Srinivasa, S. Thaakur, *Int. J. Res. Pharm. Sci*, 2012, **3**, 470.
19. Seza Ozge Gonen Melek Erol Taygun Sadriye Ku çukbayrak, *Chemical Engineering Technology*, 2015, **38**, 844-50.
20. Mashhadikhan M, Soleimani M, Parivar K, Yaghmaei P, *Journal of Medical Biotechnology*, 2015, **7**, 32-8.
21. Bei Feng, Huichuan Duan, Wei Fu, Yilin Cao, Wen Jie Zhang, Yanzhong Zhang , *J Biomed Mater Res Part A,* 2014, **103**, 431-8.
22. Nguyen Thuy Ba Linha, Young Ki Minb and Byong-Taek Lee, *Journal of Biomaterials Science*, 2013, **24**, 520–538.
23. Nguyen Thuy Ba Linh, Kap-Ho Lee, Byong-Taek Lee, *J Biomed Mater Res Part A*, 2013, **101A**, 2412–2423.
24. Nguyen Thuy Ba Linh, Young Ki Min, Ho-Yeon Song, Byong-Taek Lee, *J Biomed Mater Res Part* B*: Applied Biomaterials*, 2010, **95**, 184-91.
25. Su Yan, Li Xiaoqiang, Liu Shuiping, Wang Hongsheng, He Chuanglong, *Journal of Applied Polymer Science*, 2010, 117:542-7.
26. Hadi Hajiali, shapour shahgasempour, M reza Naimi-Jamal, Habibullah Peirovi, *International journal of Nanomedicine*, 2011, 6:2133-41.
27. Purushothaman Kuppan, Swaminathan Sethuraman and Uma Maheswari Krishnan, *Journal of Biomaterials Science,* 2014, **25**, 574–593.
28. G. Ramanathan, S. Singaravelu, M.D. Raja, S.S.L. Sobhana, U.T. Sivagnanam, J. Biomater. Tissue Eng. 2014; 4: 203-209.
29. R.M. Devendiran, S.K. Chinnaiyan, R.K. Mohanty, G. Ramanathan, S. Singaravelu, S.S.L. Sobhan, *J. Biomater. Tissue Eng*, 2014, **4**, 430.
30. S Singaravelu, G Ramanathan, Raja. M. D, Sagar Barge, Uma T S, *Materials letters*, 2015; **152**: 90.
31. Rui Zhao, Xiang Li, Bolun Sun, Yan Tong, Ziqiao Jiang and Ce Wang. *RSC Adv.,* 2015, **5**, 16940.
32. Thangavelu Muthukumar, P. Prabu, Kausik Ghosh, Thotapalli Parvathaleswar S, Colloids and Surfaces B: Biointerfaces, 2014, **113**, 207.
33. Giriprasath Ramanathan, Sivakumar Singaravelu, Raja. M. D, Uma Tiruchirapalli Sivagnanam, *Micron.* 2015. DOI: 10.1016/j.micron.2015.05.010.
34. Cuicui Wang, Zhibin Fan and Yong Han, *J. Mater. Chem. B*, 2015, **3,** 5442
35. Subramani Kandhasamy, Giriprasath Ramanathan, Jayabal Kamalraja, Ravichandran Balaji, Narayanasamy Mathivanan, Uma Tiruchirapalli Sivagnanam and Paramasivan Thirumalai Perumal, *RSC advances*, 2015, DOI: 10.1039/C5RA07133J.
36. N. Natarajan, V. Shashirekha, S. E. Noorjahan, M. Rameshkumar, C. Rose, and T. P. Sastry, *Journal of*

Macromolecular Science Part A: Pure and Applied Chemistry, 2005, **42**, 945.

37. Kansiz, M., Billman, H. and Mcnaughton, D, *Appl. Environ. Microbiol.,* 2000, **66**, 3415.
38. R. Ashokkumar, M. Ramaswamy, *Int. J. Curr. Microbiol. App. Sci,* 2014, **3**, 395.
39. Kim, G., Michler, M., Henning, G. H., Radusch, S. and Wutzler, H. J, *J. Appl. Polym. Sci.,* 2007, **103**, 1860.
40. JiaoJiao Deng, YueLong Wang, LiangXue Zhou, MaLing Gou, Na Luo, HaiFeng Chen, AiPing Tong, Chao You and Gang Guo, *RSC Adv.*, 2015 , **5**, 42943.
41. Mingzhong Lia, Masayo Ogiso, Norihiko Minoura, *Biomaterials*, 2003, **24**, 357.
42. Tao Liu, Xinbo Ding, Dongzhi Lai, Yongwei Chen, Ridong Zhang, Jianyong Chen, Xinxing Feng, Xiaoyi Chen, Xianyan Yang, Ruibo Zhao, Kai Chen and Xiangdong Kong, *J. Mater. Chem. B,* 2014, **2**, 6293.
43. Xinli Zhu, Wenguo Cui, Xiaohong Li and Yan Jin, *Biomacromolecule*s, 2008, **9**, 1795.
44. N. Nagiah, G. Ramanathan, T.S. Uma, L. Madhavi, A. R, T.S. Natarajan. *Adv. Polym. Technol*, 2013, **32,** 1.
45. Asaga, H., Klkuchl, S. and Yoshizato, K, *Exp. Cell Res, 1991,* **193**, 167-174.
46. Frederick Grinnel, TRENDS in Cell Biology. 2003, 13, 5.
47. K. Anselme, C. Bacques, G. Charriere, D.J. Hartmann, D. Herbage, R. Garrone, J. Biomed. Mater. Res., 1990, **24** 689.
48. A.E. Postlethwaite, J.M. Seyer A.H. Kang, *PNAS*, 1978, ***75***, 871.
49. Maria Moffa, Alessandro Polini, Anna Giovanna Sciancalepore, Luana Persano, Elisa Mele, Laura Gioia Passione, Giovanni Potente and Dario Pisignano, *Soft Matter,* 2013, **9**, 5529.
50. Giuseppe Vitiello, Alessandra Luchini, Gerardino DErrico, Rita Santamaria, Antonella Capuozzo, Carlo Irace,d Daniela Montesarchio and Luigi Paduano, Cationic, *J. Mater. Chem. B,* 2015, **3**, 3011.

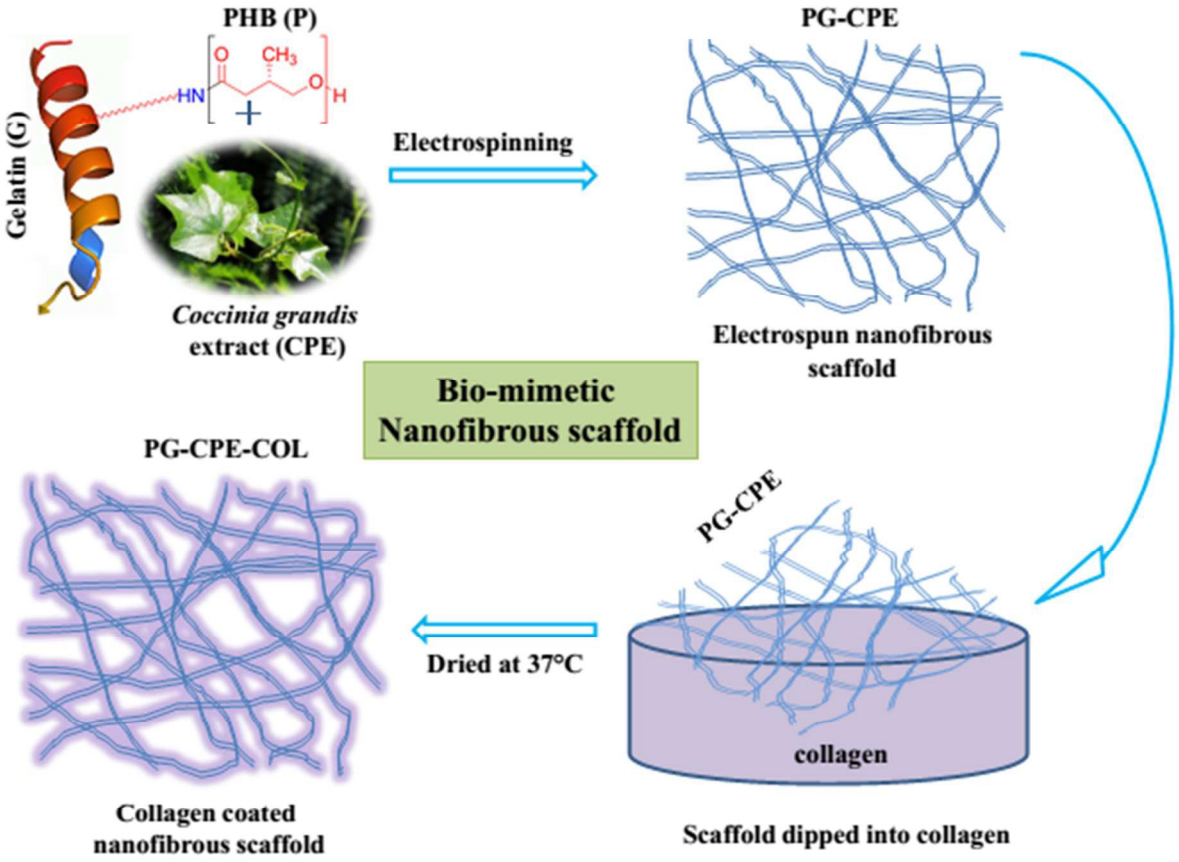

The collagen coated nanofibrous scaffold as bio-mimetic material in skin tissue engineering application was found to be simple and also easily up scalable technique due to its high surface to volume ratio. The nanofibrous scaffold mimics the function of the extra cellular matrix and aids in good biocompatibility, cell adhesion and cell proliferation. The nanofibrous scaffold coated with collagen is capable to provide as a promising tool in skin tissue engineering application.